Copper(II) coordination chemistry of potentially octadentate (N_8) tetrapyridyl and tetrapyrazolyl-pyridazine ligands. X-ray crystal structures of $[Cu_2(PTAPY)Br_4]\cdot 2DMF$ and $[Cu_2(PTAPY)(NO_3)_2(N_3)(H_2O)]_2(NO_3)_2\cdot 1.2CH_3OH$

Santokh S. Tandon*, Liqin Chen, Laurence K. Thompson, Sean P. Connors and John N. Bridson

Department of Chemistry, Memorial University of Newfoundland, St. John's, Nfld., A1B 3X7 (Canada)

(Received March 26, 1993; revised June 3, 1993)

Abstract

The structural, electrochemical, ESR and magnetic properties of a series of dinuclear copper(II) complexes of two new polyfunctional pyridazine ligands, 3,6-bis(*N,N,N',N'*-tetrakis(pyridine-2-ylmethyl)-aminoethanethiolato pyridazine (PTAPY), and 3,6-bis(*N,N,N',N'*-tetrakis(pyrazol-1-ylmethyl)-aminoethanethiolato pyridazine (PTAPZ) are discussed. PTAPY and PTAPZ are potentially octadentate (N_8) ligands and on reaction with copper(II) salts form dinuclear complexes, $[Cu_2(PTAPY)X_4]\cdot yH_2O$ ($X=NO_3$, $y=1$ (**I**); $X=Br$, $y=2$ (**II**)), $[Cu_2(PTAPY)(CH_3CN)_2](ClO_4)_4\cdot 0.5C_2H_5OH$ (**III**), $[Cu_2(PTAPZ)Cl_4]\cdot 5H_2O$ (**V**), and a tetranuclear complex $[Cu_2(PTAPY)(NO_3)_2(N_3)(H_2O)]_2(NO_3)_2\cdot 1.2CH_3OH$ (**IV**). The single crystal X-ray structures of compounds **II** and **IV** have been determined, and in each case the ligand is hexadentate. **II** ($[Cu_2(PTAPY)Br_4]\cdot 2DMF$) crystallized in the triclinic system, space group $P\bar{1}$, with $a=14.037(3)$, $b=14.941(4)$, $c=11.782(6)$ Å, $\alpha=103.77(3)$, $\beta=106.08(3)$, $\gamma=84.59(2)°$, $V=2305(2)$ Å^3 and $Z=2$ ($R=0.036$ and $R_w=0.032$). Two different five-coordinate (CuN_3Br_2) geometries exist within the same molecule. **IV** crystallized in the triclinic system, space group $P\bar{1}$, with $a=14.876(5)$, $b=16.172(4)$, $c=10.068(2)$ Å, $\alpha=95.45(2)$, $\beta=108.40(2)$, $\gamma=64.74(2)°$ and $Z=2$ ($R=0.058$ and $R_w=0.051$). The two copper atoms are quite different with six- (axially elongated, distorted tetragonal) and five- (distorted square-pyramidal) coordinate arrangements, and dimerization through azido nitrogens results in the formation of a tetranuclear azide bridged molecule. The pyridazine nitrogens remain uncoordinated in all complexes and there is no magnetic interaction between the distant copper centers. Cyclic voltammograms are characterized by the presence of either one 'two-electron' or two 'one-electron' (overlapping) reversible or quasi-reversible redox processes, associated with the reduction of the dinuclear copper(II) species to dinuclear copper(I) species.

Introduction

In recent years a substantial amount of work on the copper coordination chemistry of tetradentate (N_4) phthalazine and pyridazine and hexadentate (N_6) phthalazine ligands has been published [1–35]. These ligands have been shown to form predominantly dinuclear complexes involving a hydroxide bridge, in addition to the diazine bridge, and in some cases halogen, nitrate, sulfate and iodate can also exist as a bridge between the two closely spaced metal centers [1, 3, 6, 8, 10, 12, 16, 21, 24, 27, 29]. The hydroxo-bridged complexes exhibit moderate to strong antiferromagnetic exchange interactions between the two copper(II) centers [1, 6, 8, 10, 19, 20, 24, 25, 26–29]. The hydroxide bridge acts as an important superexchange pathway for antiferromagnetic coupling, while the diazine bridges also contribute significantly to the antiferromagnetic exchange interaction with pyridazine being more efficient than phthalazine [35].

In continuing our interest in dinuclear and polynuclear complexes of polyfunctional ligands involving diazine moieties we have examined two new ligands, PTAPY (3,6-bis(*N,N,N',N'*-tetrakis(pyridine-2-ylmethyl)-aminoethanethiolato pyridazine) and PTAPZ (3,6-bis(*N,N,N',N'*-tetrakis(pyrazol-1-ylmethyl)-aminoethanethiolato pyridazine), which are potentially octadentate (N_8) ligands (see Fig. 1), and have the potential to hold two or more metal centers in close proximity. In this paper we report the results of our investigation on the interaction of these ligands with copper(II) salts. PTAPY and PTAPZ form mainly dinuclear complexes of 2:1 metal:ligand stoichiometry. The X-ray structures of the complexes $[Cu_2(PTAPY)Br_4]\cdot 2DMF$ (**II**) and

*Author to whom correspondence should be addressed.

0020-1693/93/$6.00

$[Cu_2(PTAPY)(NO_3)_2(N_3)(H_2O)]_2(NO_3)_2 \cdot 1.2CH_3OH$ (**IV**) have been determined.

Experimental

Synthesis of ligands and copper(II) complexes

3,6-Bis(N,N,N',N'-tetrakis(pyridine-2-ylmethyl)-aminoethanethiolato pyridazine (PTAPY)

PTA [36] (5.20 g, 22.6 mmol) and 2-(chloromethyl)pyridine (14.83 g, 90.4 mmol) were dissolved in water (100 ml). A solution of sodium hydroxide (7.24 g, 181 mmol) in water (50 ml) was added dropwise to the mixture, with stirring, over a period of *c.* 1 h. The mixture was stirred for a further 12 h and the brown oil formed was extracted with dichloromethane. The extract was washed with water (3×50 ml) and dried over anhydrous sodium sulfate. After removing the dichloromethane the remaining dark brown oil was chromatographed (silica gel:hexane/$CHCl_3$) to give a pale yellow crystalline compound. Yield 6.4 g, 48%; m.p. 88–90 °C. ^1H NMR ($CDCl_3$) (δ(relative intensity)): 2.97(4) (triplet, CH_2a), 3.52(4) (triplet, CH_2b), 3.90(8) (singlet, CH_2c), 7.16(8) (multiplet, pyridinc), 7.60(8) (multiplet, pyridine), 8.50(2) (doublet, pyridazine). Mass spectrum (*m/e*) 502 (the highest mass peak corresponds to the parent ion minus one methyl-pyridine residue).

3,6-Bis(N,N,N',N'-tetrakis(pyrazol-1-ylmethyl)-aminoethanethiolato pyridazine (PTAPZ)

1-(Hydroxymethyl)pyrazole (1.80 g, 18.30 mmol) was dissolved in acetonitrile (50 ml) and PTA (1.0 g, 4.35 mmol) was then added under inert (N_2) atmosphere. After several hours PTA began to dissolve and after 2 days the solution was a clear golden yellow in color. The solvent was removed on a rotary evaporator and the product was dried further *in vacuo* to give a golden colored liquid, which from NMR study was shown to be of sufficient purity for further reactions. ^1H NMR ($CDCl_3$) (δ(relative intensity)): 7.6(4) (doublet, pyrazole-2), 7.5(4) (doublet, pyrazole-4), 7.03(2) (singlet, pyridazine), 6.28(4) (triplet, pyrazole), 5.1(8) (singlet, methylene protons attached to pyrazole), 2.9–3.5(8) (multiplet, methylene protons of PTA).

$[Cu_2(PTAPY)(NO_3)_4] \cdot H_2O$ (I)

Copper nitrate (0.36 g, 1.5 mmol) and PTAPY (0.25 g, 0.50 mmol) were dissolved in methanol (40 ml) and the reaction mixture was refluxed for 24 h. The resulting bluish green solution was concentrated to *c.* 5 ml and 40 ml of ethanol added. A bluish green solid separated, which was filtered off, washed with ethanol (3×5 ml) and dried under vacuum at room temperature for 24 h. Recrystallization from methanol/ethanol (1:1) mixture produced bluish green crystals. Yield 71%. *Anal.* Calc. for $[Cu_2(PTAPY)(NO_3)_4] \cdot H_2O$: C, 38.90; H, 3.67; N, 17.01. Found: C, 38.68; H, 3.45; N, 17.15%.

$[Cu_2(PTAPY)Br_4] \cdot 2H_2O$ (II)

A solution of PTAPY (0.25 g, 0.50 mmol) in methanol (10 ml) was added to a solution of copper bromide (0.34 g, 1.5 mmol) in 20 ml of methanol, and the reaction mixture was refluxed for 24 h. A dark grey solid separated, which was filtered off and washed with ethanol (3×5 ml). Recrystallization from a methanol/water (1:1) mixture produced green crystals. Yield 70%. *Anal.* Calc. for $[Cu_2(PTAPY)Br_4] \cdot 2H_2O$: C, 35.64; H, 3.55; N, 10.40. Found: C, 35.92; H, 3.43; N, 10.02%. Crystals used for the X-ray structure analysis were obtained as $[Cu_2(PTAPY)Br_4] \cdot 2DMF$ by the slow diffusion of ether into a DMF solution of the complex. X-ray data were collected at low temperature because the crystals crumble slowly on standing, due to solvent loss.

$[Cu_2(PTAPY)(CH_3CN)_2](ClO_4)_4 \cdot 0.5C_2H_5OH$ (III)

A solution of PTAPY (0.60 g, 1.0 mmol) in ethanol (20 ml) was added to a solution of copper perchlorate (1.1 g, 3.0 mmol) in ethanol (20 ml) and the mixture refluxed for 3 h. A blue crystalline compound formed, which was filtered off and washed with ethanol (3×5 ml). Recrystallization from an acetonitrile/ethanol (1:1) mixture produced deep blue crystals. Yield 40%. *Anal.* Calc. for $[Cu_2(PTAPY)(CH_3CN)_2](ClO_4)_4 \cdot 0.5C_2H_5OH$: C, 36.28; H, 3.04; N, 11.43. Found: C, 36.31; H, 3.58; N, 11.20%.

$[Cu_2(PTAPY)(NO_3)_2(N_3)(H_2O)]_2(NO_3)_2 \cdot 1.2CH_3OH$ (IV)

A solution of copper(II) nitrate (0.72 g, 3.0 mmol) in methanol (50 ml) was added to a solution of PTAPY (0.60 g, 1.0 mmol) in the same solvent (50 ml). A blue solution formed, which was stirred at ambient temperature for about 5 min, followed by the addition of a solution of NaN_3 (0.40 g, 6.0 mmol) in 20 ml of hot methanol. A green colored solution was produced along with a small amount of a dark brown solid. The brown solid was filtered off and discarded and the green filtrate was concentrated to 10 ml. A greenish blue solid separated, which was dissolved by adding 10 ml of DMF followed by 30 ml of methanol and the reaction mixture was refluxed for 5 min and filtered hot. The filtrate, which was allowed to stand at room temperature for several days, deposited a blue crystalline solid, which was filtered off, washed with methanol (3×3 ml) and ether (3×10 ml) and dried under vacuum at room temperature. Yield 50%. The crystals used for X-ray structure determination were obtained by the slow diffusion of ether into a solution of the complex in a

mixture of dimethyl sulfoxide/methanol/acetonitrile (1:1:1).

$[Cu_2(PTAPZ)Cl_4]\cdot 5H_2O$ (V)

PTAPZ (0.54 g, 1.0 mmol) was dissolved in methanol (20 ml) and added to an aqueous solution (10 ml) of copper chloride (0.34 g, 2.0 mmol). The green solution was allowed to evaporate in air and triethylorthoformate (1 ml) was added. A green crystalline material formed, which was filtered off and dried under vacuum for 2 h. Yield 30%. *Anal.* Calc. for $[Cu_2(PTAPZ)Cl_4]\cdot 5H_2O$: C, 31.68; H, 4.40; N, 18.50. Found: C, 31.76; H, 3.78; N, 19.06%.

Caution: Copper(II) azide and its complexes are potentially very explosive and should be prepared in small amounts.

Physical measurements

NMR spectra were recorded with a Bruker WP80 spectrometer ($SiMe_4$ internal standard), mass spectra were obtained with a VG Micromass 7070 HS spectrometer with a direct insertion probe and electronic spectra with a Cary 5E spectrometer. IR spectra were recorded as nujol mulls using a Mattson Polaris FT-IR instrument. EPR spectra were obtained using a Bruker ESP 300 X-band spectrometer at room temperature and 77 K. Room temperature magnetic susceptibilities were measured by the Faraday method using a Cahn 7600 Faraday magnetic susceptibility system.

Electrochemical measurements were performed at room temperature in dimethylformamide (DMF) (spectro-quality grade dried over molecular sieves) under O_2 free conditions using a BAS CV-27 voltammograph and a Hewlett-Packard 7005B XY recorder. For cyclic voltammetry a three electrode system was used in which the working electrode was glassy-carbon, the counter electrode platinum and with a saturated calomel (SCE) reference electrode. For constant potential electrolysis (CPE) a three component 'H' cell was used with a central 5 ml working compartment separated from auxiliary and reference compartments by medium porosity sintered glass frits. The working electrode was a platinum mesh 'flag', the auxiliary electrode a platinum wire, with a silver wire reference electrode. The supporting electrolyte was 0.1 M tetraethylammonium perchlorate (TEAP). All potentials are reported versus the saturated calomel electrode (SCE). For cyclic voltammetry all solutions were 10^{-3}–10^{-4} M in complex.

Microanalyses were carried out by Canadian Microanalytical Service, Delta, Canada.

Crystallographic data collection and refinement of the structures

$[Cu_2(PTAPY)Br_4]\cdot 2DMF$ (II)

The crystals of **II** are green. The diffraction intensities of an approximately $0.400\times0.300\times0.150$ mm crystal were collected with graphite monochromatized Mo Kα radiation using a Rigaku AFC6S diffractometer at -125 ± 1 °C and the ω–2θ scan technique to a $2\theta_{max}$ value of 50.0°. A total of 8474 reflections was measured, of which 8112 were unique and 5866 were considered significant with $I_{net} > 2.0\sigma(I_{net})$. An empirical absorption correction was applied, after a full isotropic refinement, using the program DIFABS [37], which resulted in transmission factors ranging from 0.71 to 1.00. The data were corrected for Lorentz and polarization effects. The cell parameters were obtained from the least-squares refinement of setting angles of 23 carefully centered reflections with 2θ in the range 43.94–49.06°.

The structure was solved by direct methods [38, 39]. The non-hydrogen atoms were refined anisotropically. The final cycle of full-matrix least-squares refinement was based on 5866 observed reflections ($I > 2.00\sigma(I)$) and 524 variable parameters and converged with unweighted and weighted agreement factors of $R = \Sigma||F_o| - |F_c||/\Sigma|F_o| = 0.036$ and $R_w = [(\Sigma w(|F_o| - |F_c|)^2/\Sigma w F_o^2)]^{1/2} = 0.032$, with weights based on counting statistics. The maximum and minimum peaks on the final difference Fourier map corresponded to 0.53 and -0.59 electrons/Å^3, respectively. Neutral-atom scattering factors [40] and anomalous-dispersion terms [41, 42] were taken from the usual sources. All calculations were performed with the TEXSAN [43] crystallographic software package using a VAX 3100 work station. A summary of the crystal and other data is given in Table 1 and atomic coordinates are given in Table 2. Hydrogen atom atomic coordinates (Table SI), anisotropic thermal parameters (Table SII), a full listing of bond distances and angles (Table SIII), a listing of structure factors (Table SIV) and least-squares planes (Table SV) are available, see 'Supplementary material'.

$[Cu_2(PTAPY)(NO_3)_2(N_3)(H_2O)]_2(NO_3)_2\cdot 1.2CH_3OH$ (IV)

The diffraction intensities of a blue crystal of approximate dimensions of $0.400\times0.350\times0.100$ mm were collected on a Rigaku AFC6S diffractometer, with graphite monochromatized Mo Kα radiation. The data were collected at a temperature of 25 ± 1 °C using the ω–2θ scan technique to a $2\theta_{max}$ value of 49.3°. Cell constants were obtained by the least-squares refinement of the setting angles of 24 carefully centered reflections with 2θ in the range 24.49–32.13°. A total of 5682 reflections was measured, of which 5424 were unique, and 3315 were considered significant with $I_{net} > 2.00\sigma(I_{net})$. The intensities of three representative

TABLE 1. Summary of crystal and data collection parameters for $[Cu_2(PTAPY)Br_4]\cdot 2DMF$ (**II**) and $[Cu_2(PTAPY)(NO_3)_2(N_3)(H_2O)]_2(NO_3)_2\cdot 1.2CH_3OH$ (**IV**)

	II	**IV**
Formula	$C_{38}H_{48}O_2N_{10}S_2Cu_2Br_4$	$C_{32.53}H_{38.4}N_{14}S_2O_{10}Cu_2$
Crystal size (mm)	$0.400\times0.300\times0.150$	$0.400\times350\times100$
Crystal color	green	blue
Formula weight	1187.69	987.16
Crystal system	triclinic	triclinic
Space group	$P\bar{1}$	$P\bar{1}$
a (Å)	14.037(3)	14.876(5)
b (Å)	14.941(4)	16.172(4)
c (Å)	11.782(6)	10.068(2)
α (°)	103.77(3)	95.45(2)
β(°)	106.08(3)	108.40(2)
γ (°)	84.59(2)	64.74(2)
V (Å^3)	2305(2)	2076(1)
D_{calc} (g cm^{-3})	1.711	1.579
Z	2	2
Absorption coefficient, μ (cm^{-1})	44.90	11.93
Radiation, λ (Å)	0.71069	0.71069
T (°C)	−125	25
F(000)	1184	1013
Scan type	ω–2θ	ω–2θ
Scan rate (° min^{-1})	8	8
$2\theta_{max}$ (°)	50.0	49.3
No. data collected	8474	5682
No. unique data	8112	5424
No. variables	524	559
GOF	1.62	2.44
R	0.036	0.058
R_w	0.032	0.051

reflections which were measured after every 150 reflections declined by 17%. A linear correction factor was applied to the data to account for this phenomenon. An empirical absorption correction, based on azimuthal scans of several reflections, was applied which resulted in transmission factors ranging from 0.76 to 1.00. The data were corrected for Lorentz and polarization effects.

The structure was solved by direct methods [38, 39]. The final cycle of full-matrix least-squares refinement was based on 3315 observed reflections ($(I>2.00\sigma(I))$) and 559 variable parameters and converged with final residuals of $R=0.059$ and $R_w=0.051$, with the non-hydrogen atoms refined anisotropically, and the weighting scheme based on counting statistics. Neutral atom scattering factors were taken from ref. 40. The maximum and minumum peaks on the final difference map corresponded to 0.77 and −0.60 e/Å^3, respectively. A summary of crystal data is given in Table 1 and atomic positional parameters are given in Table 3. Hydrogen atom positional parameters (Table SVI), anisotropic thermal parameters (Table SVII), a full listing of bond distances and angles (Table SVIII), a listing of structure factors (Table SIX) and least-squares planes (Table SX) are available, see 'Supplementary material'.

Results and discussion

The scheme for the synthesis of the ligands is shown in Fig. 1. The synthetic starting material for the ligands is 3,6-di(aminoethanethiolato)pyridazine (PTA), which should be capable of binding two metals, in its own right, in the same manner as the tetradentate (N_4), pyridazine and phthalazine ligands [1–8, 9–27, 29–31, 33–35]. However PTA is difficult to prepare and handle and is susceptible to decomposition. If PTA is exposed to air for a long period of time a polymeric material of unknown composition is formed, which is insoluble in most common solvents. PTA will form copper complexes readily, but they are unstable and undergo spontaneous reduction with the formation of what appear to be non-stoichiometric, mixed oxidation state species. As a consequence these complexes are difficult to characterize. However open chain and macrocyclic ligands [36, 44], which are formed from PTA, and their complexes, have much greater stability. PTAPZ is somewhat unstable and very low yields of complexes are produced if the reaction mixtures are heated. The ligands PTAPY and PTAPZ do not give molecular ions in their mass spectra, giving only fragments resulting from sulfur–carbon bond cleavage, suggesting an inherent

TABLE 2. Final atomic positional parameters and equivalent isotropic temperature factors with e.s.d.s in parentheses for $[Cu_2(PTAPY)Br_4]\cdot 2DMF$ (**II**)

Atom	x	y	z	B_{eq}[a]
Br(1)	0.92466(4)	−0.12477(4)	0.58120(6)	2.92(2)
Br(2)	0.77330(4)	0.03992(4)	0.80738(5)	2.21(2)
Br(3)	0.22311(4)	0.46102(4)	0.02607(5)	2.69(2)
Br(4)	0.16901(4)	0.53921(4)	0.36566(5)	2.93(2)
Cu(1)	0.83850(4)	0.02027(4)	0.61574(5)	1.67(2)
Cu(2)	0.22870(4)	0.41497(4)	0.22271(6)	1.80(2)
S(1)	0.3987(1)	0.0990(1)	−0.0208(1)	2.22(5)
S(2)	0.8243(1)	0.2180(1)	0.2670(1)	2.48(6)
O(1)	0.7148(3)	0.6678(3)	0.4107(4)	3.6(2)
O(2)	0.4082(3)	0.7227(3)	0.2250(4)	3.3(2)
N(1)	0.9610(3)	0.0974(3)	0.7006(3)	2.1(2)
N(2)	0.7866(3)	0.1423(3)	0.5648(3)	1.5(2)
N(3)	0.7055(3)	−0.0209(3)	0.5014(3)	1.7(2)
N(4)	0.6335(3)	0.1901(3)	0.2439(4)	2.0(2)
N(5)	0.5391(3)	0.1646(3)	0.1799(4)	2.0(2)
N(6)	0.1029(3)	0.3469(3)	0.1533(4)	1.9(2)
N(7)	0.2863(3)	0.2812(3)	0.2339(4)	1.7(2)
N(8)	0.3713(3)	0.4440(3)	0.2968(3)	1.7(2)
N(9)	0.8453(3)	0.5752(3)	0.3697(4)	2.4(2)
N(10)	0.4506(4)	0.6492(3)	0.0532(4)	3.1(2)
C(1)	1.0547(4)	0.0669(4)	0.7375(5)	3.0(2)
C(2)	1.1330(4)	0.1285(5)	0.7860(5)	3.9(3)
C(3)	1.1130(5)	0.2215(5)	0.7946(5)	4.2(3)
C(4)	1.0160(5)	0.2534(4)	0.7574(5)	3.4(3)
C(5)	0.9417(4)	0.1884(4)	0.7110(4)	2.3(2)
C(6)	0.8341(4)	0.2153(3)	0.6703(4)	2.1(2)
C(7)	0.6775(4)	0.1439(3)	0.5369(4)	2.1(2)
C(8)	0.6419(4)	0.0488(3)	0.4736(4)	1.6(2)
C(9)	0.5480(4)	0.0319(4)	0.3958(4)	2.3(2)
C(10)	0.5177(4)	−0.0585(4)	0.3489(5)	2.8(2)
C(11)	0.5822(4)	−0.1290(4)	0.3801(5)	2.7(2)
C(12)	0.6755(4)	−0.1078(4)	0.4538(5)	2.4(2)
C(13)	0.8210(4)	0.1406(3)	0.4547(4)	1.7(2)
C(14)	0.8166(4)	0.2335(3)	0.4203(4)	1.9(2)
C(15)	0.7022(4)	0.1854(3)	0.1858(5)	2.0(2)
C(16)	0.6839(4)	0.1551(4)	0.0597(5)	2.4(2)
C(17)	0.5911(4)	0.1301(4)	−0.0034(4)	2.3(2)
C(18)	0.5192(4)	0.1358(3)	0.0612(5)	1.9(2)
C(19)	0.3329(4)	0.1344(3)	0.0949(4)	1.9(2)
C(20)	0.3109(4)	0.2387(3)	0.1165(4)	1.8(2)
C(21)	0.0186(4)	0.3768(4)	0.0846(5)	2.4(2)
C(22)	−0.0601(4)	0.3194(4)	0.0230(5)	2.9(2)
C(23)	−0.0514(4)	0.2288(4)	0.0324(5)	2.9(2)
C(24)	0.0342(4)	0.1976(4)	0.1070(5)	2.6(2)
C(25)	0.1096(4)	0.2589(4)	0.1675(4)	2.0(2)
C(26)	0.2046(4)	0.2344(3)	0.2510(5)	2.2(2)
C(27)	0.3766(4)	0.2929(3)	0.3372(4)	2.0(2)
C(28)	0.4301(4)	0.3755(3)	0.3383(4)	1.7(2)
C(29)	0.5315(4)	0.3849(4)	0.3836(5)	2.3(2)
C(30)	0.5729(4)	0.4664(4)	0.3889(5)	2.6(2)
C(31)	0.5128(4)	0.5372(4)	0.3475(4)	2.1(2)
C(32)	0.4118(4)	0.5229(3)	0.3008(4)	1.9(2)
C(33)	0.7525(5)	0.6048(4)	0.3502(6)	3.4(3)
C(34)	0.9175(4)	0.6204(4)	0.4773(5)	3.5(3)
C(35)	0.8778(5)	0.4910(4)	0.2972(5)	4.0(3)
C(36)	0.3866(4)	0.6803(4)	0.1202(6)	3.0(3)
C(37)	0.4193(6)	0.6060(5)	−0.0753(6)	6.1(4)
C(38)	0.5547(5)	0.6679(4)	0.1029(6)	4.0(3)

[a] $B_{eq} = \frac{8\pi^2}{3}\sum_{i=0}^{3}\sum_{j=0}^{3} U_{ij}a^*_i a^*_j \vec{a}_i \cdot \vec{a}_j$.

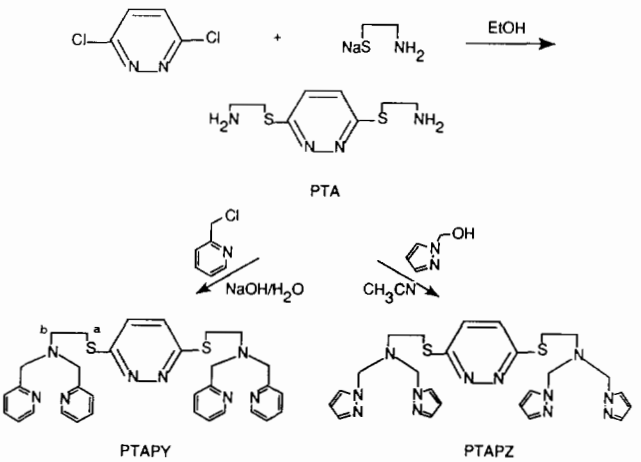

Fig. 1. Scheme for the synthesis of the ligands.

TABLE 3. Final atomic positional parameters and equivalent isotropic temperature factors with e.s.d.s in parentheses for $[Cu_2(PTAPY)(NO_3)_2(N_3)(H_2O)]_2(NO_3)_2\cdot 1.2CH_3OH$ (**IV**)

Atom	x	y	z	B_{eq}[a]
Cu(1)	0.26723(9)	0.39820(8)	0.8735(1)	4.19(8)
Cu(2)	0.9548(1)	0.04530(7)	0.6491(1)	3.85(8)
S(1)	0.4335(2)	0.0638(2)	0.6347(3)	5.7(2)
S(2)	0.8790(2)	0.0429(2)	0.8730(3)	4.2(2)
O(1)	0.2183(5)	0.4797(5)	1.0197(7)	6.4(5)
N(1)	0.1267(6)	0.4052(5)	0.770(1)	4.1(5)
N(2)	0.3003(6)	0.3398(5)	0.6966(7)	3.9(5)
N(3)	0.4106(6)	0.3870(5)	0.926(1)	4.4(5)
N(4)	0.5723(6)	0.1349(5)	0.7221(8)	4.2(6)
N(5)	0.6716(6)	0.1297(5)	0.7732(7)	3.7(5)
N(6)	1.1042(6)	0.0038(5)	0.7569(7)	3.7(5)
N(7)	0.9464(6)	0.1702(5)	0.7252(8)	3.8(5)
N(8)	0.8076(6)	0.1150(5)	0.5417(7)	3.5(5)
N(9)	0.9749(6)	−0.0752(5)	0.5676(8)	3.7(6)
N(10)	0.9327(8)	−0.1144(7)	0.579(1)	7.4(9)
N(11)	0.887(1)	−0.1611(8)	0.562(1)	9(1)
C(1)	0.049(1)	0.4217(6)	0.822(1)	5.2(7)
C(2)	−0.0477(8)	0.4253(7)	0.739(2)	5.8(8)
C(3)	−0.061(1)	0.4085(8)	0.600(2)	6(1)
C(4)	0.019(1)	0.3905(7)	0.545(1)	5.3(8)
C(5)	0.1115(8)	0.3900(6)	0.632(1)	4.4(7)
C(6)	0.2005(8)	0.3780(7)	0.582(1)	5.4(7)
C(7)	0.3811(9)	0.3661(7)	0.682(1)	5.2(8)
C(8)	0.4521(8)	0.3702(6)	0.821(1)	4.5(7)
C(9)	0.551(1)	0.3578(7)	0.839(1)	6(1)
C(10)	0.611(1)	0.3656(8)	0.972(2)	8(1)
C(11)	0.572(1)	0.3827(8)	1.082(1)	7(1)
C(12)	0.472(1)	0.3937(7)	1.054(1)	5.7(9)
C(13)	0.3410(7)	0.2381(6)	0.717(1)	3.8(6)
C(14)	0.3576(7)	0.1840(7)	0.588(1)	5.1(7)
C(15)	0.5601(7)	0.0572(7)	0.702(1)	3.7(7)
C(16)	0.6421(9)	−0.0283(7)	0.734(1)	4.4(7)
C(17)	0.7418(8)	−0.0339(6)	0.786(1)	4.2(7)
C(18)	0.7514(7)	0.0505(7)	0.8045(8)	3.4(7)
C(19)	0.8515(8)	0.1649(7)	0.889(1)	5.9(9)
C(20)	0.934(1)	0.1835(7)	0.868(1)	6.3(9)
C(21)	1.1762(9)	−0.0798(7)	0.796(1)	4.1(7)

(*continued*)

TABLE 3. (*continued*)

Atom	*x*	*y*	*z*	B_{eq}[a]
C(22)	1.280(1)	−0.1012(8)	0.864(1)	5.3(8)
C(23)	1.3106(9)	−0.031(1)	0.897(1)	6(1)
C(24)	1.239(1)	0.0575(8)	0.861(1)	5.3(8)
C(25)	1.1370(8)	0.0727(7)	0.792(1)	4.2(7)
C(26)	1.0515(9)	0.1665(7)	0.743(1)	4.8(8)
C(27)	0.8609(8)	0.2379(6)	0.616(1)	4.6(7)
C(28)	0.7763(8)	0.2079(7)	0.548(1)	4.0(7)
C(29)	0.675(1)	0.2684(7)	0.488(1)	5.2(8)
C(30)	0.5999(8)	0.2356(8)	0.421(1)	5.1(8)
C(31)	0.6309(8)	0.1430(7)	0.415(1)	4.3(7)
C(32)	0.7333(9)	0.0874(6)	0.476(1)	3.7(7)
O(3)	0.453(1)	0.191(1)	1.067(1)	22(2)
O(4)	0.374(1)	0.2140(9)	1.211(1)	16(1)
O(5)	0.2935(6)	0.2725(6)	1.0064(9)	8.4(7)
N(12)	0.376(1)	0.2268(8)	1.089(2)	10(1)
O(6)	0.1975(7)	0.5626(6)	0.7403(9)	8.4(7)
O(7)	0.1461(7)	0.6483(6)	0.898(1)	9.9(8)
O(8)	0.149(1)	0.7060(7)	0.716(1)	13(1)
N(13)	0.1649(8)	0.6402(9)	0.781(1)	8(1)
O(9)	0.7070(7)	0.4334(6)	0.737(1)	8.1(7)
O(10)	0.652(1)	0.4821(7)	0.529(1)	15(1)
O(11)	0.6585(8)	0.5720(6)	0.690(1)	12(1)
N(14)	0.6691(9)	0.4954(8)	0.648(1)	6.6(9)
O(2)	0.129(1)	0.2553(8)	0.069(1)	7(1)
C(33)	0.113(2)	0.305(1)	0.181(2)	7(2)

[a] $B_{eq} = \frac{8\pi^2}{3} \sum_{i=0}^{3} \sum_{j=0}^{3} U_{ij} a^*_i a^*_j \vec{a}_i \cdot \vec{a}_j$.

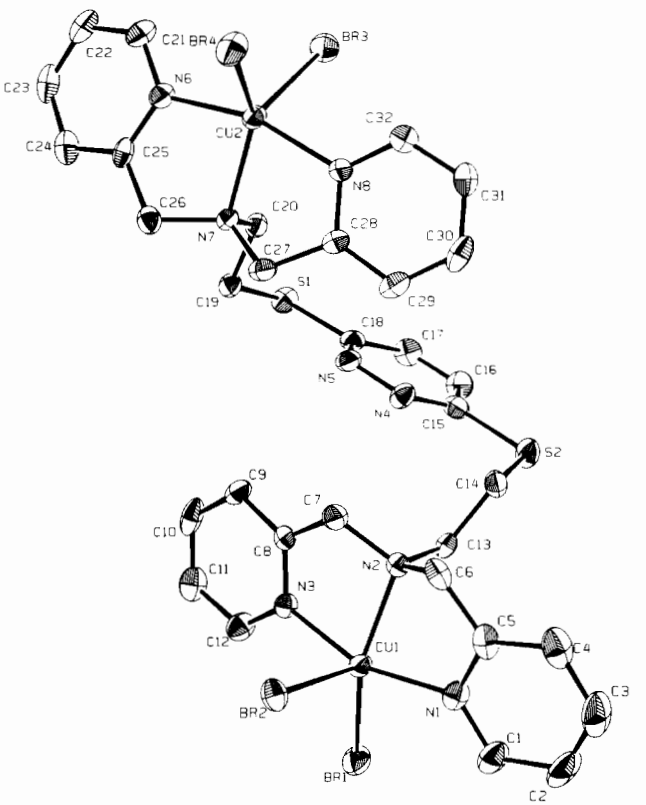

Fig. 2. Structural view of $[Cu_2(PTAPY)Br_4]$ (**II**), with hydrogen atoms omitted.

instability for these ligands. However supporting evidence for the ligand structures came from ^1H NMR spectra and C, H, N analyses of their complexes and the X-ray crystal structures in the case of PTAPY.

Description of the X-ray crystal structures of $[Cu_2(PTAPY)Br_4]\cdot 2DMF$ *(II) and* $[Cu_2(PTAPY)(NO_3)_2(N_3)(H_2O)]_2(NO_3)_2\cdot 1.2CH_3OH$ *(IV)*

A perspective view of **II** is shown in Fig. 2, and selected bond distances and angles relevant to the copper coordination spheres are given in Table 4. Each copper ion is bonded to two pyridine nitrogen atoms, a tertiary amine nitrogen atom and two bromine atoms in distorted five-coordinate arrangements. However the two copper centers are quite different. The stereochemistry at Cu(I) can best be described as a distorted square pyramid with four short in-plane contacts involving pyridine nitrogens (N(1), N(3)), amine nitrogen (N(2)) and a bromine atom (Br(1)) and a weak axial interaction with a long copper–bromine bond (2.608 Å), which is somewhat shorter than those reported for other, related five-coordinate square pyramidal copper(II) complexes involving axially bound bromine [24, 30]. Cu(1) is displaced by 0.429(4) Å from the mean plane of the four in-plane donors, N(1), N(2), N(3), Br(1) towards the apical bromine atom Br(2). The

TABLE 4. Interatomic distances (Å) and angles (°) relevant to the copper coordination spheres in $[Cu_2(PTAPY)Br_4]\cdot 2DMF$ (**II**)

Br(1)–Cu(1)	2.384(1)	Br(2)–Cu(1)	2.608(1)
Br(3)–Cu(2)	2.549(2)	Br(4)–Cu(2)	2.447(1)
Cu(1)–N(1)	2.040(4)	Cu(1)–N(2)	2.060(4)
Cu(1)–N(3)	2.027(4)	Cu(2)–N(6)	1.991(4)
Cu(2)–N(7)	2.104(4)	Cu(2)–N(8)	1.993(4)
Cu(1)–Cu(2)	7.406(2)		
Br(1)–Cu(1)–Br(2)	109.82(4)	Br(1)–Cu(1)–N(1)	96.6(1)
Br(1)–Cu(1)–N(2)	149.8(1)	Br(1)–Cu(1)–N(3)	96.9(1)
Br(2)–Cu(1)–N(1)	95.8(1)	Br(2)–Cu(1)–N(2)	100.3(1)
Br(2)–Cu(1)–N(3)	92.8(1)	N(1)–Cu(1)–N(2)	80.6(2)
N(1)–Cu(1)–N(3)	160.5(2)	N(2)–Cu(1)–N(3)	80.6(2)
Br(3)–Cu(2)–Br(4)	112.44(4)	Br(3)–Cu(2)–N(6)	94.0(1)
Br(3)–Cu(2)–N(7)	115.1(1)	Br(3)–Cu(2)–N(8)	94.0(1)
Br(4)–Cu(2)–N(6)	97.2(1)	Br(4)–Cu(2)–N(7)	132.4(1)
Br(4)–Cu(2)–N(8)	94.4(1)	N(6)–Cu(2)–N(7)	81.2(2)
N(6)–Cu(2)–N(8)	162.2(2)	N(7)–Cu(2)–N(8)	81.0(2)

stereochemistry at Cu(2) can best be described as a distorted trigonal bipyramid. The axial ligands (N(6), N(8)) form an almost linear arrangement about the copper center (Cu(2)) with an angle N(6)–Cu(2)–N(8) of 162.2°. Equatorial angles of 115.1, 112.44 and 132.4° are reasonable for a distorted trigonal bipyramid, and this is supported by the fact that the two equatorial copper bromine distances (2.549(2), 2.447(1) Å) com-

pare more closely than in the case of the square pyramidal copper center. The copper–copper separation is 7.406(2) Å, clearly indicating no possible intradimer association between the copper centers. The copper–nitrogen (pyridine) contacts (1.991–2.040 Å) are in the range reported for these coordination geometries in copper(II) complexes with related ligands [45]. The $Cu–N_{amino}$ bond lengths differ significantly with Cu(1)–N(2) (2.060(4) Å) and Cu(2)–N(7) (2.104(4) Å) lying in the range found in other structurally similar dinuclear copper(II) complexes [45] and in a series of copper(II) mononuclear complexes with tertiary amine ligands located in the basal plane of the tetragonal pyramid [46, 47]. The pyridazine nitrogen atoms remain uncoordinated and the two copper centers are held apart at two ends of the ligand by the two tripodal N_3 chromophores. Two DMF molecules are present in the asymmetric unit and are not bonded to the metal centers.

The structure of complex **IV** is shown in Figs. 3 and 4, which illustrate the monomeric, dinuclear unit and the dimeric tetranuclear unit, respectively. Bond lengths and angles relevant to the copper coordination spheres are listed in Table 5. The structures of compounds **II** and **IV** are similar in that the two metallic centers are located at the ends of the ligand, but in **IV** the distance of separation between the copper atoms (10.228(4) Å), is much longer than in **II**. In compound **IV**, the two copper centers are quite different with a five- and a six-coordinate stereochemistry. Cu(1) has a distorted tetragonal structure with four short in-plane contacts involving pyridine nitrogens (N(1), N(3)), amino nitrogen (N(2)) and an oxygen atom from a water molecule. The long axial contacts, which differ significantly (Cu(1)–O(5) 2.363(8), Cu(1)–O(6) 2.717(9) Å) involve

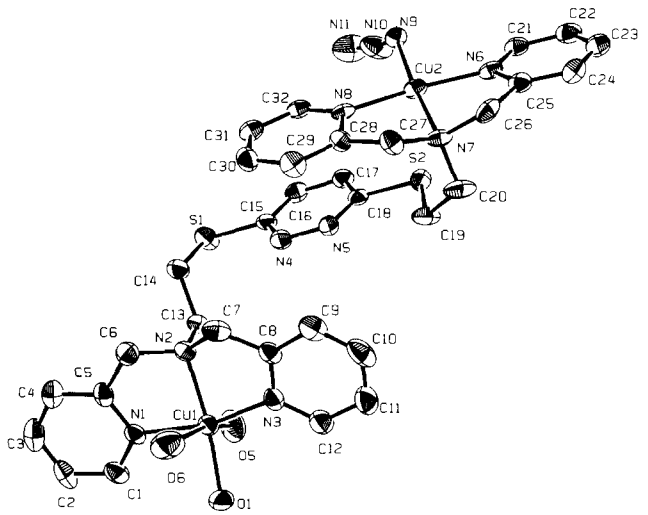

Fig. 3. Structural view of the monomeric, dinuclear unit $[Cu_2(PTAPY)(NO_3)_2(N_3)(H_2O)]$ (**IV**), with hydrogen atoms and nitrates omitted.

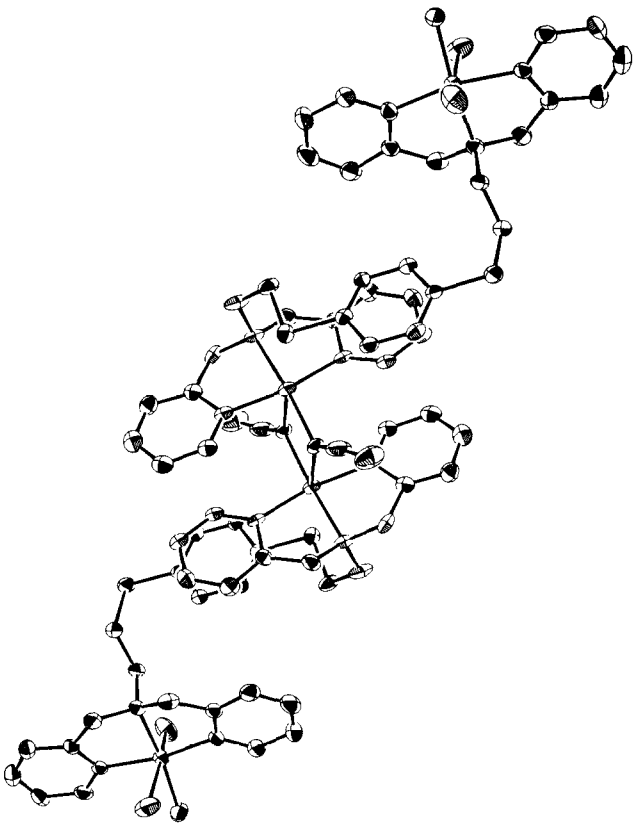

Fig. 4. Structural view of the dimeric tetranuclear complex $[Cu_2(PTAPY)(NO_3)_2(N_3)(H_2O)]_2$ (**IV**), with hydrogen atoms and nitrates omitted.

TABLE 5. Interatomic distances (Å) and angles (°) relevant to the copper coordination spheres in $[Cu_2(PTAPY)(NO_3)_2(N_3)(H_2O)]_2(NO_3)_2 \cdot 1.2CH_3OH$ (**IV**)

Cu(1)–O(1)	1.980(6)	Cu(1)–N(1)	1.979(8)
Cu(1)–N(2)	2.036(7)	Cu(1)–N(3)	1.959(8)
Cu(2)–N(6)	1.978(8)	Cu(2)–N(7)	2.058(7)
Cu(2)–N(8)	1.966(8)	Cu(2)–N(9)	1.978(8)
Cu(1)–O(5)	2.363(8)	Cu(1)–O(6)	2.717(9)
Cu(2)–N(9)[a]	2.857(9)	Cu(1)–Cu(2)	10.228(5)
Cu(2)–Cu(2)[a]	3.607(3)		
O(1)–Cu(1)–N(1)	93.3(3)	O(1)–Cu(1)–N(2)	167.6(3)
O(1)–Cu(1)–N(3)	99.9(3)	N(1)–Cu(1)–N(2)	82.9(3)
N(1)–Cu(1)–N(3)	164.7(4)	N(2)–Cu(1)–N(3)	82.6(3)
O(6)–Cu(1)–O(5)	166.8(3)	N(9)–Cu(2)–N(9)[a]	85.3(3)
N(6)–Cu(2)–N(7)	83.0(3)	N(6)–Cu(2)–N(8)	166.3(3)
N(6)–Cu(2)–N(9)	93.4(3)	N(7)–Cu(2)–N(8)	84.5(3)
N(7)–Cu(2)–N(9)	173.7(3)	N(8)–Cu(2)–N(9)	98.5(3)
Cu(2)–N(9)–Cu(2)[a]	94.7(3)		

[a]Symmetry code: $2-x, -y, 1-z$.

the oxygen atoms of two monodentate nitrate groups, one of which is clearly weakly coordinated. The copper center is displaced by 0.160(8) Å from the mean plane of the four in-plane donors (N_3O) towards the axial nitrate O(5). The stereochemistry at Cu(2) can best be described as distorted square pyramidal involving

two pyridine nitrogens (N(6), N(8)), amino nitrogen (N(7)) and azido nitrogen (N(9)) in the basal plane, all with contacts <2.06 Å, and with a very weak axial interaction to an azido nitrogen atom (Cu(2)–N(9) 2.857(9) Å) from another dinuclear molecule resulting in the formation of a weakly associated tetranuclear, dimeric structure. This weak bridging association creates an unusual asymmetric azide bridged structure, in which the two copper centers are linked by an equatorial (short) and an axial (long) azide bond. The copper center (Cu(2)) is displaced by 0.101(7) Å from the mean plane of the four in-plane donors (N(6), N(7), N(8), N(9)), towards apical azido nitrogen atom (N(9)). Non-stoichiometric solvent (methanol) was found in the unit cell, but is not bonded to the metal centers.

Spectroscopic properties

The IR spectra of compounds **I–IV** are similar in the spectral region where ligand absorptions are observed. The spectra for bulk samples of **II** and **IV** are almost identical to their recrystallized (X-ray) samples, except for a strong band at 1669 cm^{-1} in **II**, corresponding to lattice DMF. Compound **I** exhibits two bands at 1742 and 1727 cm^{-1} associated with the combination bands ($\nu_1 + \nu_4$) of the nitrate groups, suggesting their monodentate behavior [48]. Compound **III** exhibits strong absorptions at 1091 and 623 cm^{-1} due to ν_3 and ν_4 modes, respectively, of ionic perchlorate and two sharp νCN absorptions at 2315 and 2286 cm^{-1} associated with coordinated acetonitrile. In copper and silver complexes involving pyridazinophane ligands, which have been shown to contain uncoordinated lattice acetonitrile, νCN bands occur at lower energies (2293, 2253 cm^{-1} (Ag); 2297, 2253 cm^{-1} (Cu)) [49, 50]. However in the complex $([Cu(DPP)(H_2O)(CH_3CN)](ClO_4)_2 \cdot 2H_2O)_x$ (DPP = 4,6-di-(2′-pyridylthio)-pyrimidine) [51], involving coordinated acetonitrile, νCN bands occur at higher energies (2301, 2273 cm^{-1}), comparable with those observed for **III**. In compound **IV** (X-ray sample) a strong band at 2044 cm^{-1} is assigned to the coordinated azido group [52] and a major nitrate combination band is observed at 1744 cm^{-1}, with weak shoulders at 1737 and 1725 cm^{-1} [48]. The band at 1744 cm^{-1} corresponds to ionic nitrate, while the low energy shoulders are associated with the monodentate nitrates. In the far-IR region compound **V** exhibits strong absorptions at 280 and 245 cm^{-1} due to terminal Cu–Cl and Cu–N stretching modes, respectively.

The electrical conductivities of millimolar solutions of compounds **I–V** were measured in DMF (Table 6). The conductance values for compounds **I**, **II** and **IV** (Table 6) lie in the range 128–168 Ω^{-1} cm^2 mol^{-1}, which is characteristic for 2:1 electrolytes [53], and suggests the partial displacement of coordinated anions by DMF molecules. The conductance value of 336 Ω^{-1} cm^2 mol^{-1} for compound **III** is indicative of 4:1 electrolytic behavior, as expected, and the conductance value of 276 Ω^{-1} cm^2 mol^{-1} for compound **V** suggests the replacement of either three or all four chlorine atoms by DMF molecules.

The solid state electronic spectra of compounds **I** and **V** exhibit one broad visible d–d absorption, while **II**, **III** and **IV** show two prominent bands, which are more typical of the presence of two different copper ion stereochemistries rather than lower symmetry ligand field components. The spectra of **II** and **IV** are certainly consistent, in this regard, with structural data, which show the presence of two different copper centers in each compound. Such a situation may also exist in compound **III**. More intense, high energy bands are clearly charge transfer in nature and may be associated with ligand to metal charge transfer. In DMF solutions shifts in the positions of the solid state bands are observed for all compounds (Table 6), suggesting changes in the metal ion coordination spheres, consistent with solvent coordination, as indicated by the conductance measurements. The general IR and electronic spectral similarities between compounds **I–IV** suggests dinuclear structures for **I** and **III**, which are similar to **II** and **IV**, and involve metal centers bound at the ligand extremities, with no pyridazine coordination. It is reasonable to assume that **V** has a similar structure to **II**, involving a hexadentate ligand, and with coordinated chloride and five-coordinate copper centers.

The electrochemical properties of compounds **I–V**, have been studied by cyclic voltammetry in DMF solutions containing 0.1 M TEAP as supporting electrolyte at a glassy carbon working electrode. Data, including $E_{1/2}$ values and peak to peak separations, are given in Table 6 and cyclic voltammograms for **II** and **IV** are shown in Figs. 5 and 6, respectively. Cyclic voltammograms for **I** and **II** are very similar and involve one almost reversible redox process at a potential around 0.0 V (versus SCE), associated with a one-step reduction of the dinuclear copper(II) species to a dinuclear copper(I) species. The cyclic voltammograms of **III** and **IV** (Fig. 6) are characterized by the presence of two quasi-reversible, overlapping redox processes at negative potentials ($E_{1/2}{}^1 = -0.015$ V (**III**), -0.02 V (**IV**); $E_{1/2}{}^2 = -0.115$ V (**III**), -0.145 V (**IV**) (versus SCE), suggesting two stepwise, one-electron reductions proceeding through a Cu(II)–Cu(I) intermediate to a dinuclear Cu(I) species. The observation of two closely separated redox processes would be consistent with the presence of two slightly different copper centers in solution, which is in agreement with the solid state structural evidence for **IV**. The cyclic voltammograms for **V** show two chemically irreversible waves at $E_{1/2}{}^1 = 0.17$ V and $E_{1/2}{}^2 = -0.06$ V (versus SCE). The current

TABLE 6. Magnetic, spectral, conductance and electrochemical data

Complex	μ_{eff} (μ_B)[a]	$\lambda_{max.}$ (nm) (ϵ)[b]	$E_{1/2}$(V) (vs SCE)[e] (ΔE_p (mV))	Conductance[d] (Ω^{-1} cm^2 mol^{-1})
$[Cu_2(PTAPY)(NO_3)_4]\cdot H_2O$ (**I**)	1.84	670, 330[c] 655 (340)[d]	0.0 (160)	147
$[Cu_2(PTAPY)Br_4]\cdot 2H_2O$ (**II**)	1.83	920, 725, 345[c] [970] (280), [850] (400) 785 (440)[d]	0.06 (100)	168
$[Cu_2(PTAPY)(CH_3CN)_2](ClO_4)_4\cdot 0.5EtOH$ (**III**)	1.88	680, [600], 330[c] 830 (130), 645 (380)[d]	−0.015 (70) −0.115 (70)	336
$[Cu_2(PTAPY)(NO_3)_2(N_3)(H_2O)]_2(NO_3)_2\cdot 1.2CH_3OH$ (**IV**)	1.73	660, [610], 385, 325[c] 630 (310), 395 (2280)[d]	−0.02 (100) −0.145 (130)	155
$[Cu_2(PTAPZ)Cl_4]\cdot 5H_2O$ (**V**)	1.95	670, 335[c] [845] (20), 690 (60)[d]	0.17, −0.06	276
Ferrocene			0.455 (90) 0.395 (90)[f]	

[a]At room temperature. [b]ϵ(dm^3 mol^{-1} cm^{-1}); [] shoulder. [c]Solid (mull transmittance). [d]DMF solutions. [e]DMF/0.1 M TEAP/GC/SCE at scan rate of 100 mV/s. [f]DMF/0.1 M TEAP/GC/Ag at scan rate of 100 mV/s.

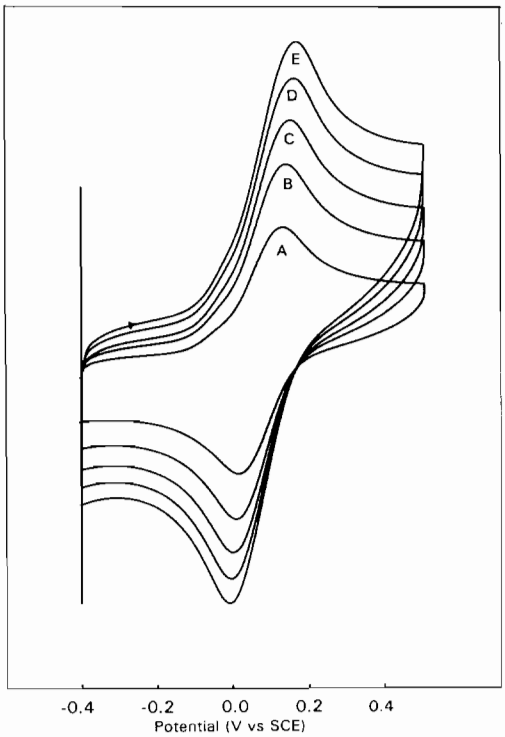

Fig. 5. Cyclic voltammograms for **II** (A–D; 100–500 mV s^{-1}).

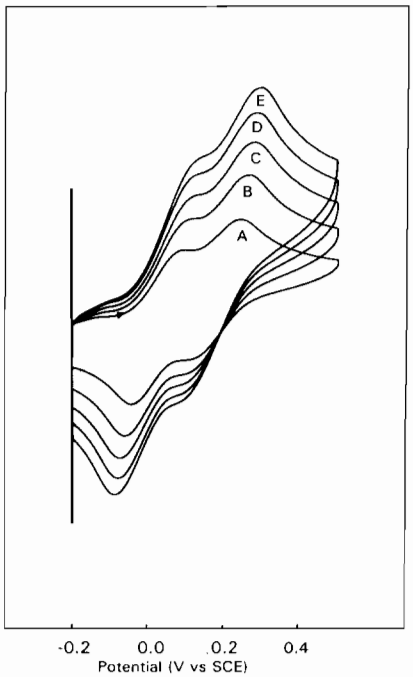

Fig. 6. Cyclic voltammograms for **IV** (A–D; 100–500 mV s^{-1}).

heights associated with these waves are quite different ($E^1 > E^2$), and an oxidation wave at +0.28 V dominates the return sweep. This suggests a structural rearrangement on oxidation to produce an oxidized species different from the starting material, unlike the situation observed for **III** and **IV**.

Controlled potential electrolysis was carried out for compounds **II** and **III** in DMF at a platinum working electrode. Reduction for **II** at −0.25 V (versus Ag) led to a change in color from bluish green to yellow,

with the passage of two equivalents of charge. Oxidation of the reduced solution at +0.70 V restored the green color and required two equivalents of charge. The yellow, reduced solution also became oxidized on exposure to air forming a green solution. Similar treatment of a blue solution of **III** at −0.55 V required two equivalents of charge to form a yellow solution, and a two-electron oxidation at +0.4 V restored the blue color.

Room temperature magnetic moments for compounds **I–III** and **V** fall in the range μ_{eff} 1.83–1.95 BM/Cu (Table 6), which is typical for mononuclear copper(II) compounds, thus suggesting the absence of any type of magnetic interactions between the two copper(II) centers. This has been confirmed by the X-ray structure determination of compound **II**, in which the two copper centers are widely separated (7.406 Å), without any short bridge linking them together, which could propagate a spin interaction. It is reasonable to assume that in these dinuclear complexes each copper behaves independently, with structures similar to that in **II**. The room temperature magnetic moment for **IV** (1.73 BM/Cu) is lower than that observed in the other compounds, and although it is nominally equal to the spin only value for a dilute copper(II) species some axial spin interaction may exist between the two dinuclear halves. The interaction is, however, likely to be weak, because of the orthogonal axial/equatorial bridging arrangement linking the two copper centers, and the fact that the axial distances are very long. However we await a variable temperature magnetic study to confirm this suggestion. Typically azide acts as a μ_2-1,1 bridge in dinuclear copper complexes, with equatorial bonding and short Cu–N distances. This bridging mode leads to ferromagnetic coupling in the few documented cases [54–58].

X-band EPR spectra of complexes **I–V** were recorded on powdered solids or solutions (DMF) at room temperature (295 K) and at liquid nitrogen temperature (77 K). **I** exhibits an axial signal in the solid state, both at room temperature and 77 K, which can be interpreted in terms of a distorted trigonal bipyramidal species with $g_{\parallel}=2.04$ and $g_{\perp}=2.14$ (295 K) (Fig. 7). In DMF solution, both at room temperature and in frozen glass at 77 K, two sets of hyperfine lines indicate the presence of two different axial species. At 77 K the hyperfine splittings of 200 and 164 G are too large for a trigonal bipyramidal species and so it appears that in solution **I** probably forms a tetragonal or distorted square pyramidal species, in which the two copper centers are different, and involves solvent coordination (1:2 electrolyte in DMF). In the solid state at room temperature a powdered sample of **II** (X-ray sample) exhibits an orthorhombic signal (Fig. 8) ($g_1=2.208$, $g_2=2.114$, $g_3=2.032$), consistent with the five-coordinate geometries indicated from the structural determination

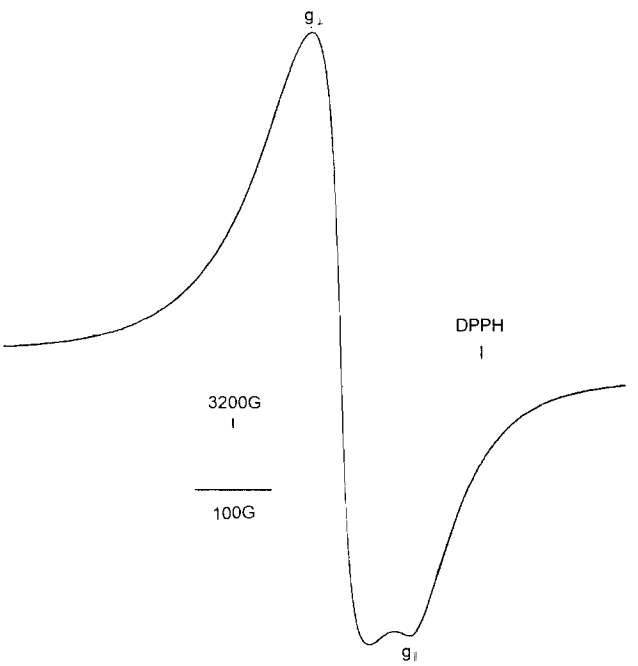

Fig. 7. Solid state EPR spectrum for a powdered sample of $[Cu_2(PTAPY)(NO_3)_4]\cdot H_2O$ (**I**) (9.76 GHz; 295 K).

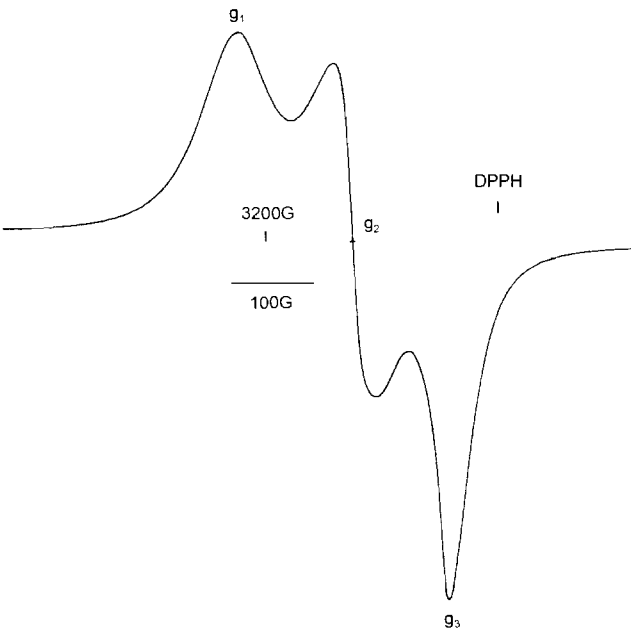

Fig. 8. Solid state EPR spectrum for a powdered sample of $[Cu_2(PTAPY)Br_4]\cdot 2DMF$ (**II**) (9.77 GHz; 295 K).

[59]. At 77 K a somewhat broadened signal is observed at $g=2.18$. Solution EPR spectra of **II**, both at room temperature and 77 K, exhibit only one broad signal centered at $g=2.10$–2.12.

III exhibits only one isotropic signal in the solid state, both at room temperature and 77 K centered at $g_0=2.06$. In DMF at 77 K **III** shows two overlapping sets of

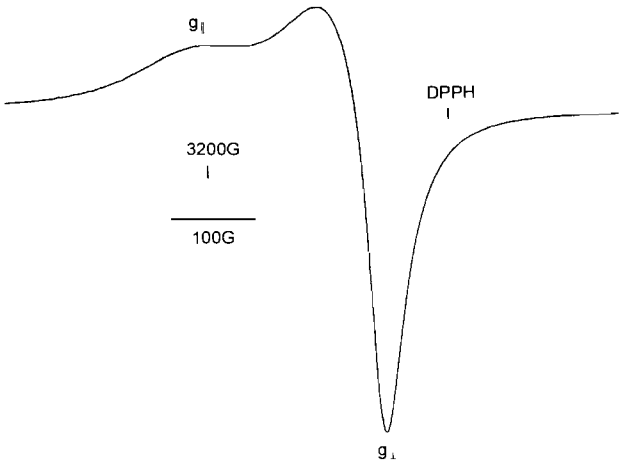

Fig. 9. Solid state EPR spectrum for a powdered sample of $[Cu_2(PTAPY)(NO_3)_2(N_3)(H_2O)]_2(NO_3)_2 \cdot 1.2CH_3OH$ (**IV**) (9.77 GHz; 295 K).

signals in the parallel region, with small and comparable hyperfine coupling constants (approx. 130 G). Although establishing g values was difficult, because of incomplete resolution of the lines, the small coupling constants suggest copper centers with appreciable tetrahedral distortion, which would be consistent with the N_4 coordination environment proposed for this complex.

The room temperature EPR spectra of both solid bulk and recrystallized samples of **IV** are identical and typical of axially elongated tetragonal species with $g_{\parallel} = 2.194$ and $g_{\perp} = 2.052$ (Fig. 9), consistent with the X-ray structure, which shows the presence of axially elongated tetragonal and square pyramidal stereochemistries at the Cu(1) and Cu(2) centers, respectively. At 77 K an identical solid state spectrum is observed. In DMF solution a broad isotropic signal is observed at both 295 and 77 K. **V** exhibits an essentially isotropic signal in the solid state spectrum ($g_0 = 2.07$) at room temperature and at 77 K ($g_0 = 2.08$), with some hyperfine resolution in the parallel region ($A_{\parallel} = \approx 180$ G) at 295 K suggestive of square pyramidal copper centers. In frozen glass in DMF at 77 K two different axial species appear to be present ($A_{\parallel} = 150$, 180 G), indicative of square pyramidal rather than trigonal bipyramidal species in solution.

Conclusions

In this paper, the synthesis, spectroscopic, magnetic and electrochemical properties of dinuclear copper(II) complexes with two new polydentate, dinucleating ligands have been discussed. PTAPY and PTAPZ, although potentially octadentate (N8) dinucleating ligands, react with copper(II) salts to form dinuclear complexes (**I**–**V**) of 2:1 (M:L) stoichiometry. The copper centers in the dinuclear molecules (**II** and **IV**) are widely separated without any magnetic interaction between them, due to the lack of involvement of the pyridazine nitrogens in coordination. The pendant N_3 donor group clearly binds strongly to copper(II) and it is not clear why all eight nitrogens are not involved in coordination simultaneously. Steric crowding and the formation of seven-membered chelate rings may prevent pyridazine coordination, a feature observed in some macrocyclic ligands based on PTA [36, 44]. In **IV** dimerization leads to the formation of a tetranuclear complex involving azido bridges.

Supplementary material

Tables of atomic coordinates for hydrogen atoms, a complete listing of bond lengths and bond angles, anisotropic thermal parameters, least-squares planes and calculated and observed structure factors are available on request from the authors.

Acknowledgement

We thank the Natural Science and Engineering Research Council of Canada for financial support for this study and for funds to purchase the Rigaku AFC6S X-ray diffractometer.

References

1 L.K. Thompson, V.T. Chacko, J.A. Elvidge, A.B.P. Lever and R.V. Parish, *Can. J. Chem., 47* (1969) 4141.
2 J.C. Dewan and L.K. Thompson, *Can. J. Chem., 60* (1982) 121.
3 D.V. Bautista, J.C. Dewan and L.K. Thompson, *Can. J. Chem., 60* (1982) 2583.
4 G. Marongiu and E.C. Lingafelter, *Acta Crystallogr., Sect. B, 38* (1982) 620.
5 G. Bullock, F.W. Hartstock and L.K. Thompson, *Can. J. Chem., 61* (1983) 57.
6 L.K. Thompson, *Can. J. Chem., 61* (1983) 579.
7 F.W. Hartstock and L.K. Thompson, *Inorg. Chim. Acta, 72* (1983) 227.
8 L.K. Thompson, F.W. Hartstock, P. Robichaud and A.W. Hanson, *Can. J. Chem., 62* (1984) 2755.
9 P. Robichaud and L.K. Thompson, *Inorg. Chim. Acta, 85* (1984) 137.
10 L.K. Thompson, A.W. Hanson and B.S. Ramaswamy, *Inorg. Chem., 23* (1984) 2459.
11 L.K. Thompson, F.W. Hartstock, L. Rosenberg and T.C. Woon, *Inorg. Chim. Acta, 97* (1985) 1.
12 M. Ghedini, G. De Munno, G. Denti, A.M. Manotti Lanfredi and A. Tiripicchio, *Inorg. Chim. Acta, 57* (1982) 87.
13 P. Dapporto, G. De Munno, G. Bruno and M. Romeo, *Acta Crystallogr., Sect. C, 39* (1983) 718.

14 A. Tiripicchio, A.M. Manotti Lanfredi, M. Ghedini and F. Neve, *J. Chem. Soc., Chem. Commun.,* (1983) 97.
15 G. De Munno, G. Denti and P. Dapporto, *Inorg. Chim. Acta, 74* (1983) 199.
16 G. De Munno and G. Denti, *Acta Crystallogr., Sect. C, 40* (1984) 616.
17 G. De Munno and G. Bruno, *Acta Crystallogr., Sect. C, 40* (1984) 2022.
18 P. Dapporto, G. De Munno, A. Sega and C. Meali, *Inorg. Chim. Acta, 83* (1984) 171.
19 S.K. Mandal, L.K. Thompson and A.W. Hanson, *J. Chem. Soc., Chem. Commun.,* (1985) 1709.
20 L.K. Thompson, T.C. Woon, D.B. Murphy, E.J. Gabe, F.L. Lee and Y. Le Page, *Inorg. Chem., 24* (1985) 4719.
21 T.C. Woon, R. McDonald, S.K. Mandal, L.K. Thompson, S.P. Connors and A.W. Addison, *J. Chem. Soc., Dalton Trans.,* (1986) 2381.
22 S.K. Mandal, L.K. Thompson, M.J. Newlands, F.L. Lee, Y. Le Page, J.-P. Charland and E.J. Gabe, *Inorg. Chim. Acta, 122* (1986) 199.
23 L.K. Thompson and T.C. Woon, *Inorg. Chim. Acta, 111* (1986) 45.
24 L.K. Thompson, S.K. Mandal, E.J. Gabe, F.L. Lee and A.W. Addison, *Inorg. Chem., 26* (1987) 657.
25 L.K. Thompson, S.K. Mandal, L. Rosenberg, F.L. Lee and E.J. Gabe, *Inorg. Chim. Acta, 133* (1987) 81.
26 S.K. Mandal, L.K. Thompson, E.J. Gabe, F.L. Lee and J.P. Charland, *Inorg. Chem., 26* (1987) 2384.
27 S.K. Mandal, T.C. Woon, L.K. Thompson, M.J. Newlands and E.J. Gabe, *Aust. J. Chem., 39* (1986) 1007.
28 L.K. Thompson, S.K. Mandal, E.J. Gabe and J.-P. Charland, *J. Chem. Soc., Chem. Commun.,* (1986) 1537.
29 L.K. Thompson, F.L. Lee and E.J. Gabe, *Inorg. Chem., 27* (1988) 39.
30 L.K. Thompson, S.K. Mandal, J.-P. Charland, and E.J. Gabe, *Can. J. Chem., 66* (1988) 348.
31 S.K. Mandal, L.K. Thompson, E.J. Gabe, J.-P. Charland and F.L. Lee, *Inorg. Chem., 27* (1988) 855.
32 S.K. Mandal, L.K. Thompson, M.J. Newlands, J.-P. Charland and E.J. Gabe, *Inorg. Chim. Acta, 178* (1990) 169.
33 P. Lacroix, O. Kahn, L. Valade, P. Cassoux and L.K. Thompson, *Synth. Met., 39* (1990) 81.
34 F. Abraham, M. Lagrenee, S. Sueur, B. Mernari and C. Bremard, *J. Chem. Soc., Dalton Trans.,* (1991) 1443.
35 S.S. Tandon, L.K. Thompson and R.C. Hynes, *Inorg. Chem., 31* (1992) 2210.
36 S.S. Tandon, L.K. Thompson and J.N. Bridson, *Inorg. Chem., 32* (1993) 32.
37 N. Walker and D. Stuart, *Acta Crystallogr., Sect. A, 39* (1983) 158.
38 C.J. Gilmore, *J. Appl. Crystallogr., 17* (1984) 42.
39 P.T. Beurskens, DIRDIF, *Tech. Rep. 1984/1,* Crystallography Laboratory, Toernooiveld, 6525 Ed Nijmegen, Netherlands, 1984.
40 D.T. Cromer and J.T. Waber, *International Tables for X-ray Crystallography,* Vol. IV, Kynoch, Birmingham, UK, 1974, Table 2.2A.
41 J.A. Ibers and W.C. Hamilton, *Acta Crystallogr., 17* (1974) 781.
42 D.T. Cromer, *International Tables for X-ray Crystallography,* Vol. IV, Kynoch, Birmingham, UK, 1974, Table 2.3.1.
43 *Texsan-Texray Structure Analysis Package,* Molecular Structure Corporation, The Woodlands, TX, 1985.
44 S.S. Tandon, L.K. Thompson, J.N. Bridson and M. Bubenik, *Inorg. Chem.,* in press.
45 (a) K.D. Karlin, J.C. Hayes, Y. Gultneh, R.W. Cruse, J.W. McKeown, J.P. Hutchinson and J. Zubieta, *J. Am. Chem. Soc., 106* (1984) 2121; (b) K.D. Karlin, P.L. Dahlstrom, S.N. Cozzette, P.M. Scensny and J. Zubieta, *J. Chem. Soc., Chem. Commun.,* (1981) 881; (c) T.N. Sorrell, M.R. Malachowski and D.L. Jameson, *Inorg. Chem., 21* (1982) 3250; (d) M.S. Nasir, K.D. Karlin, D. McGowty and J. Zubieta, *J. Am. Chem. Soc., 113* (1991) 698.
46 J. Zubieta, K.D. Karlin and J.C. Hayes, in K.D. Karlin and J. Zubieta (eds.), *Copper Coordination Chemistry: Biochemical & Inorganic Perspectives,* Adenine, Guilderland, NY, 1983, pp. 97–108.
47 K.D. Karlin, J.C. Hayes, S. Juen, J.P. Hutchinson and J. Zubieta, *Inorg. Chem., 21* (1982) 4106.
48 A.B.P. Lever, E. Mantovani and B.S. Ramaswamy, *Can. J. Chem., 49* (1971) 1957.
49 L. Chen, L.K. Thompson and J.N. Bridson, *Can. J. Chem., 70* (1992) 1886.
50 L. Chen, L.K. Thompson and J.N. Bridson, *Can. J. Chem., 70* (1992) 2709.
51 L. Chen, L.K. Thompson and J.N. Bridson, unpublished results.
52 R. Cortes, J.I. Ruiz de Larramendi, L. Lezama, T. Rojo, K. Urtiaga and M.I. Arriortua, *J. Chem. Soc., Dalton Trans.,* (1992) 2723.
53 W.J. Geary, *Coord. Chem. Rev., 7* (1971) 81.
54 O. Kahn, *Inorg. Chim. Acta, 62* (1982) 3.
55 J. Cormarmond, P. Plumeré, J.-M. Lehn, Y. Agnus, R. Louis, R. Weiss, O. Kahn and I. Morgenstern-Badarau, *J. Am. Chem. Soc., 104* (1982) 6330.
56 O. Kahn, S. Sikorav, J. Gouteron, S. Jeannin and Y. Jeannin, *Inorg. Chem., 22* (1983) 1877.
57 S. Sikorav, I. Bkouche-Waksman and O. Kahn, *Inorg. Chem., 23* (1984) 490.
58 S.S. Tandon, L.K. Thompson and J.N. Bridson, *J. Chem. Soc., Chem. Commun.,* (1993) 804.
59 T. Rojo, J.I.R. Larramendi, I. Duran, J.L. Mesa, J. Via and M.I. Arriortua, *Polyhedron, 22* (1990) 2693.